

[CONTRIBUTION FROM THE DEPARTMENT OF CHEMISTRY, THE PENNSYLVANIA STATE UNIVERSITY, UNIVERSITY PARK, PA.]

## The Reaction of Methyl Radicals with Nitric Oxide

BY A. MASCHKE, B. S. SHAPIRO, AND F. W. LAMPE

RECEIVED OCTOBER 14, 1963

Methyl- $d_3$  radicals, formed by the photolysis of azomethane- $d_6$ , react with nitric oxide by successive addition to form trimethylhydroxylamine- $d_9$ . During this successive addition, nitrosomethane- $d_3$  is the sole product observed until nitric oxide consumption is essentially complete. Thereafter the successive addition of radicals to nitrosomethane- $d_3$  to form trimethylhydroxylamine- $d_9$  is in competition with ethane- $d_6$  formation by radical combination. A kinetic analysis of the data subsequent to nitric oxide consumption leads to a lower limit of  $6.51 \times 10^{-14}$  cm.<sup>3</sup> molecule<sup>-1</sup> sec.<sup>-1</sup> for the reaction  $CD_3 + CD_3NO \rightarrow (CD_3)_2NO$ .

In a recent communication<sup>1</sup> we reported some observations on the sequence of reactions occurring when methyl- $d_3$  radicals were formed by the room temperature photolysis of azomethane- $d_6$  in the presence of low concentrations (ca. 0.2–2%) of nitric oxide. It was shown that under these conditions nitrosomethane- $d_3$  is formed exclusively until depletion of nitric oxide is essentially complete. After the nitric oxide is consumed, trimethylhydroxylamine- $d_9$  and ethane- $d_6$  are formed in competing processes, the former presumably by successive addition of methyl- $d_3$  radicals to nitrosomethane- $d_3$  and the latter by methyl- $d_3$  radical combination. These findings were consistent with the work of Phillips<sup>2</sup> and Bromberger and Phillips<sup>3</sup> who found trimethylhydroxylamine as a product in their studies of the methyl radical abstraction of nitric oxide from methyl nitrite at 180°. The reaction sequence reported earlier<sup>1</sup> is also in agreement with Hoare's<sup>4</sup> recent studies of the acetone–nitric oxide photolysis at 200° in which it was found that between two and three methyl radicals were scavenged per nitric oxide molecule. Moreover, the reaction sequence found in the gas phase<sup>1</sup> appears to be analogous to the findings of Gingras and Waters,<sup>5</sup> that in solution three 2-cyano-2-propyl radicals add to each nitric oxide molecule.

This paper comprises a more complete report of our studies of the reaction sequence in the room temperature photolysis of azomethane- $d_6$ –nitric oxide mixtures.

### Experimental

Methyl- $d_3$  radicals were generated by the photolysis of azomethane- $d_6$  with light of wave length greater than 3100 Å. The photolyses were carried out at room temperature (ca. 25°) in a cylindrical cell, in one end of which was a gold-foil having a pin-hole leak into the ionization chamber of a Bendix Model 14-101 Time-of-Flight mass spectrometer. The opposite end consisted of a flat quartz window for admission of the light beam while the cylindrical wells were constructed of stainless steel. The apparatus is entirely similar to that described in detail by Heicklen and Johnston<sup>6</sup> except that we used a smaller pinhole (diameter of ~0.002 in.) and only a 3-l. reactant reservoir. We found that, with the time constant of 690 sec. of this pin hole leak, pressure diminution of reactants in the 3-l. reservoir was always less than 5% over the course of photolysis. Azomethane- $d_6$  was used to avoid the mass interference of nitric oxide and ethane at  $m/e$  30.

In the first experiments the entire mass range up to  $m/e$  100 was repeatedly scanned during photolysis. After the identity of product peaks had been established, the photolyses were conducted by continuously monitoring each product peak and the parent peak of azomethane- $d_6$  ( $m/e$  64) simultaneously. The simul-

taneous measurement of the azomethane- $d_6$  parent peak and the various product peaks permitted the use of peak height ratios (product peak height to  $m/e$  64) to determine product concentrations. Over the course of a photolysis the azomethane- $d_6$  concentration remains essentially constant<sup>1</sup> so that the ratio technique corrects for small fluctuations in electron beam current and electron multiplier sensitivity. In general, the mass spectrometer was operated with an ionizing electron energy of 50 e.v. and an electron trap current of 0.15  $\mu$ a. A few experiments were conducted with a nominal electron energy of 18 e.v.

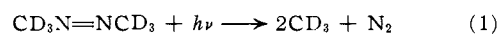
The light source was an Osram HBO-109 high-pressure mercury arc which has a low wave length cut-off at about 3100 Å. The spectral emission of the lamp and the wave length dependence of the azomethane absorption coefficient are such that the average effective wave length is about 3660 Å. The power supply to the lamp was of such a nature that reproducibility of the lamp current and, hence, of the incident intensity, was  $\sim \pm 20\%$ .

Nitric oxide that had been obtained from the Matheson Co. was used as received. Azomethane- $d_6$ , stated to have an isotopic purity of greater than 99%, was obtained from Merck Sharpe and Dohme, Ltd. Although this was received and stored in a darkened container, it was always found necessary to remove traces of the photolysis products ethane- $d_6$  and nitrogen before each set of photolyses. This was accomplished by several freeze–pump–thaw cycles using a freezing methanol slush as the cooling bath.

A direct calibration of  $m/e$  36 from ethane- $d_6$  was not possible as the compound was not on hand. Instead we obtained the parent peak height–concentration relationship for ethane- $d_6$  using  $m/e$  33 from 1,1,2-ethane- $d_3$ . This introduces no significant error into our results because the ionic abundance of  $m/e$  33 from 1,1,2-ethane- $d_3$  is within 2% of that of  $m/e$  36 from ethane- $d_6$ ,<sup>7</sup> and no significant (*i.e.* >1%) differences in total ionization cross section are to be expected.

### Results and Discussion

**Photolysis of Pure Azomethane.**—When pure azomethane- $d_6$  is photolyzed under our conditions, the only products observed are nitrogen and ethane- $d_6$ . The formation of ethane- $d_6$  is indicated by the growth of  $m/e$  36, the observation of which suffers no interference from the mass spectral peaks of azomethane- $d_6$ . The formation of nitrogen is evident from the growth of the residual  $m/e$  28 after corrections for the contributions from azomethane- $d_6$  and ethane- $d_6$  are made. Although we looked specifically for methane- $d_4$  and radical addition products of the  $CD_3N=N$  radical, such products were present only at concentrations below the limit of our detection sensitivity. With ethane- $d_6$  and nitrogen being the only products observed, we can write for the photolysis mechanism of azomethane- $d_6$  under these conditions



Methyl- $d_3$  radicals are at a concentration level much below our sensitivity of detection. Hence, in a kinetic treatment of our flow system we need not consider

(1) A. Maschke, B. S. Shapiro, and F. W. Lampe, *J. Am. Chem. Soc.*, **85**, 1876 (1963).

(2) L. Phillips, *Proc. Chem. Soc.*, 204 (1961).

(3) B. Bromberger and L. Phillips, *J. Chem. Soc.*, 5302 (1961).

(4) D. E. Hoare, *Can. J. Chem.*, **40**, 2012 (1962).

(5) B. A. Gingras and W. A. Waters, *J. Chem. Soc.*, 1920 (1954).

(6) J. Heicklen and H. S. Johnston, *J. Am. Chem. Soc.*, **84**, 4394 (1962).

(7) J. A. Bell and G. B. Kistiakowsky, *ibid.*, **84**, 3417 (1962).

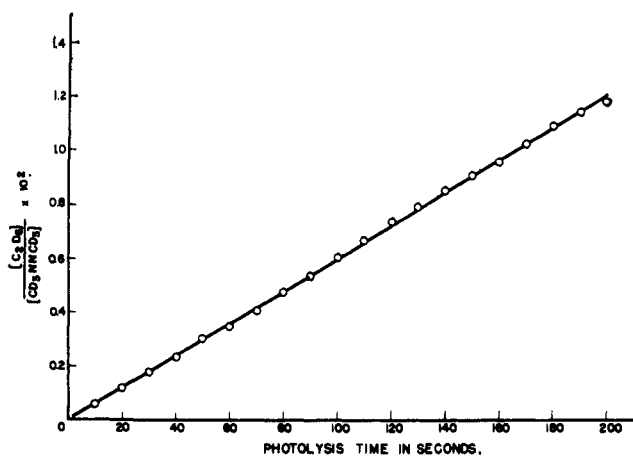


Fig. 1.—Formation of ethane- $d_6$  in photolysis of pure azomethane- $d_6$  at 11.3 mm.

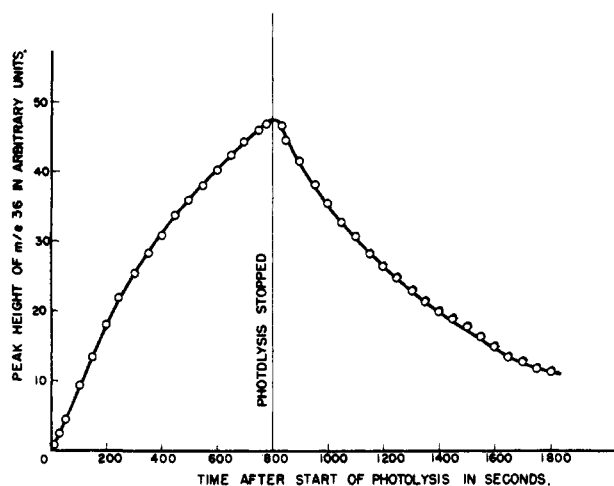


Fig. 2.—Approach to steady state and first-order decay of ethane- $d_6$  in photolysis of pure azomethane- $d_6$  ( $\sim 12$  mm.).

their leakage rate through the pinhole but rather may consider them to be at a steady state concentration determined by 1 and 2. Such an assumption leads to the following expression for the rate of formation of ethane- $d_6$  in the photolysis of pure azomethane- $d_6$

$$d[C_2D_6]/dt = \phi\alpha I_0[CD_3N=NCD_3] - \lambda[C_2D_6] \quad (E1)$$

where  $\phi$  is the primary quantum yield of azomethane- $d_6$  photodissociation,  $\alpha$  is the average absorption coefficient,  $I_0$  is the effective light flux emitted by the lamp, and  $\lambda$  is the specific leakage rate through the pinhole. Since the azomethane- $d_6$  concentration is essentially constant over a run, (E1) is easily integrated to give

$$\frac{[C_2D_6]}{[CD_3N=NCD_3]} = \frac{\phi I_0 \alpha}{\lambda} (1 - e^{-\lambda t}) \quad (E2)$$

Thus the  $[C_2D_6]/[CD_3N=NCD_3]$  ratio approaches a steady state value ( $t = \infty$ ) of  $\phi I_0 \alpha / \lambda$ , while in the limit of zero time

$$[C_2D_6]/[CD_3N=NCD_3] \Rightarrow \phi I_0 \alpha t \quad (E3)$$

In Fig. 1 is shown a plot of the  $[C_2D_6]/[CD_3N=NCD_3]$  ratio as a function of time for the early part of a photolysis at an azomethane- $d_6$  pressure of 11.3 mm. This plot bears out (E3) and further leads to a value of  $6.02 \times 10^{-5}$  sec. $^{-1}$  for the quantity  $\phi I_0 \alpha$ . The approach to the steady state can be seen, for  $t < 800$  sec.,

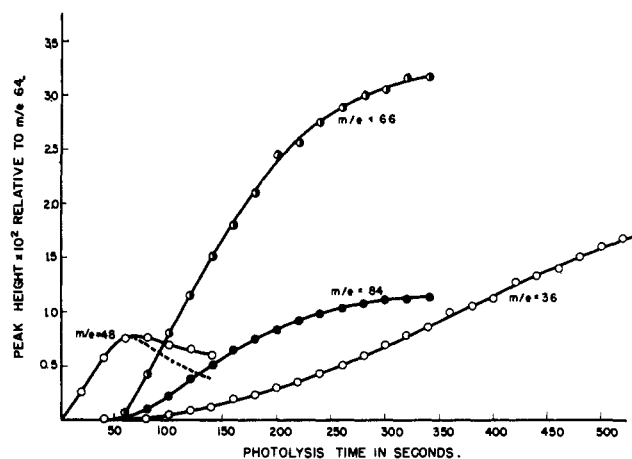


Fig. 3.—Photolysis of azomethane- $d_6$ -nitric oxide mixture; azomethane- $d_6$  pressure, 12.3 mm.; initial pressure nitric oxide, 0.08 mm.

in Fig. 2 in which the peak height of  $m/e$  36 in arbitrary units is plotted vs. photolysis time. At  $t = 800$  sec. the light was shut off in order to follow the decay of  $m/e$  36 and measure  $\lambda$ . According to (E1) when  $I_0 = 0$  we have a first-order decay with a specific rate of  $\lambda$  (sec. $^{-1}$ ), and hence  $\lambda$  can be determined as the slope of a plot of the logarithm of the peak height vs. time. Such a plot of the data in Fig. 2 for  $t < 800$  sec. is nicely linear and gives  $\lambda = 1.45 \times 10^{-3}$  sec. $^{-1}$  or a time constant for the leak of 690 sec.

As pointed out by Hecklen and Johnston,<sup>6</sup> the mean free path of the gas molecules is small compared with the diameter of the pinhole, and under such conditions the flow is not molecular but viscous so that the low concentration products are simply swept through by the reactants. Hence, the time constant of the leak should be approximately the same for all product molecules.<sup>8</sup>

The combination of  $\phi\alpha I_0$  and  $\lambda$ , according to (E2) at  $t = \infty$ , shows that under our conditions the steady state concentration ratio of a product to azomethane- $d_6$  is  $4.1 \times 10^{-2}$ .

**Photolysis of Azomethane- $d_6$ -Nitric Oxide Mixtures.**—When mixtures of azomethane- $d_6$  and nitric oxide (at 0.2 to 2 mole %) are photolyzed, the only product peak observed in the initial stages is  $m/e$  48. This mass peak, which undoubtedly corresponds to  $CD_3NO$ , goes through a maximum and then slowly decreases, and only near this maximum and subsequent to it are other product mass peaks observed. This can be clearly seen in Fig. 3, where the ratios of product mass-peak heights to  $m/e$  64 (the parent ion of azomethane- $d_6$ ) are plotted vs. photolysis time. Thus, near the maximum of  $m/e$  48, peaks of  $m/e$  36, 66, and 84 make their appearance. The peak at  $m/e$  36 is undoubtedly due to ethane- $d_6$  whose initial formation is apparently inhibited by the presence of nitric oxide. Indeed, the maximum slope of the growth curve of  $m/e$  36 is, within the experimental error of resetting the lamp current, equal to the formation rate of  $m/e$  36 in the pure azomethane- $d_6$  photolysis. Thus, the first conclusion to be drawn from Fig. 3 is that nitric oxide completely inhibits ethane formation until late in the photolysis, but that eventually the ethane formation rate reaches its

(8) Measurement of the leak rate of  $C_2H_{10}$  formed by the combination of ethyl radicals leads to a time constant of  $\sim 700$  sec. If the flow were molecular, this measurement would have yielded  $\sim 880$  sec.

completely uninhibited value. The decrease of  $m/e$  48 near the time at which the other product peaks appear suggests that  $CD_3NO$  can no longer form because the NO is, for all practical purposes, consumed; further it suggests that the  $CD_3NO$  is destroyed by  $CD_3$  radicals, which in the virtual absence of NO can react with it to form products that yield mass peaks at  $m/e$  66 and 84 and can react with each other to form ethane- $d_6$ . In addition, the similar nature of the growth curves of  $m/e$  66 and 84 is indicative that they are mass spectral peaks coming from the same compound. No other product mass peaks were found, although we specifically looked for peaks characteristic of  $(CD_3NO)_2$ ,<sup>9a,b</sup>  $(CD_3)_2N-N(CD_3)_2$ ,<sup>10</sup> and further addition products of  $CD_3NO$  with NO.<sup>11</sup> Neither  $m/e$  66 nor 84 is characteristic of the known and expected mass spectra of these possible products. These findings are in apparent conflict with the results of Coe and Doumani<sup>9a</sup> and Calvert, Thomas, and Hanst<sup>9b</sup> who found only  $CH_3NO$  and  $(CH_3NO)_2$ . This apparent disagreement, which is a result of quite different experimental conditions, warrants some discussion.

First, in contrast to these earlier reports<sup>9a,b</sup> no crystals of  $(CD_3NO)_2$  were visible, although the vessel was thoroughly inspected by eye. Second, if  $(CD_3NO)_2$  were formed under our conditions it would have been observable at  $m/e$  96. Collin<sup>12</sup> has observed  $(CH_3NO)_2^+$  in appreciable abundance (11%) in the mass spectrum of nitrosomethane and has thus demonstrated that: (1) the dimer has sufficient vapor pressure and stability to be introduced into the ionization chamber of a mass spectrometer; and (2) the dimeric ion  $(CD_3NO)_2^+$  has sufficient stability to be observed mass spectrometrically. Thus, since  $(CD_3NO)_2$  would be within our detection and measurement capability, we can only conclude that under our conditions the dimer is not formed.

This is not too surprising a conclusion when one considers the competing reaction paths available to  $CD_3NO$ . These are: (1) Leakage through the pinhole with a first-order specific reaction rate of  $1.45 \times 10^{-3}$  sec.<sup>-1</sup>; (2) dimerization by reaction with another  $CD_3NO$  molecule, a reaction for which Calvert, Thomas, and Hanst<sup>9b</sup> have estimated a second-order specific reaction rate of  $1.5 \times 10^{-19}$  cm.<sup>3</sup>/molecule sec.; and (3) reaction with  $CD_3$  radicals with a specific reaction rate (as shown later)  $>6.5 \times 10^{-14}$  cm.<sup>3</sup>/molecule sec. Even at the highest  $CD_3NO$  concentration observed in our experiments the dimerization rate was only of the order of 0.6 of the leak rate through the pinhole. On the other hand, the rate of reaction of  $CD_3NO$  with  $CD_3$  was in all cases several times to an order of magnitude faster than the leakage rate.

Thus in our studies, which employed low NO concentrations (0.2–2%) and continuous photolysis of azomethane- $d_6$ , the dimerization reaction is negligible. In the work of Calvert, Thomas, and Hanst,<sup>9b</sup> however, high NO concentrations (39–72%) were employed and the dimerization kinetics were studied with the photolysis stopped. In these experiments,<sup>9b</sup> therefore, the presence of NO during photolysis would keep the steady

state  $CH_3$  concentration so low as to favor dimerization of  $CH_3NO$  rather than reaction with  $CH_3$ , while in their observation of the dimerization reaction with the light off, the  $CH_3$  concentration is zero and dimerization would be the only reaction path available for  $CH_3NO$ . Thus in our work the low concentration of NO results in a steady state  $CD_3$  concentration sufficiently high to favor the reaction of  $CD_3NO$  with  $CD_3$  to form  $(CD_3)_2NOCD_3$  over the dimerization of  $CD_3NO$ . Under the conditions used by Calvert, Thomas, and Hanst<sup>9b</sup> the dimerization reaction occurs almost exclusively.

Bromberger and Phillips,<sup>3</sup> who identified trimethylhydroxylamine as a product in studies of the  $CH_3-CH_3ONO$  reaction, have synthesized this product and reported its mass spectrum. In Table I is a comparison of the mass spectrum reported by Bromberger and Phillips<sup>3</sup> for  $(CH_3)_2NOCH_3$  and the relative peak heights of  $m/e$  66 and 84 found in our work.

TABLE I  
COMPARISON OF PRODUCT PEAK RATIO WITH MASS SPECTRUM OF TRIMETHYLHYDROXYLAMINE

—(CH <sub>3</sub> ) <sub>2</sub> NOCH <sub>3</sub> —			—(CD <sub>3</sub> ) <sub>2</sub> NOCD <sub>3</sub> (?)—		
<i>m/e</i>	Ion	Rel. intensity	<i>m/e</i>	Ion	Rel. intensity
30	NO <sup>+</sup>	11.4	30	NO <sup>+</sup>	...
45	CH <sub>3</sub> NO <sup>+</sup>	15.2	48	CD <sub>3</sub> NO <sup>+</sup>	...
60	(CH <sub>3</sub> ) <sub>2</sub> NO <sup>+</sup>	100.0	66	(CD <sub>3</sub> ) <sub>2</sub> NO <sup>+</sup>	100.0
75	(CH <sub>3</sub> ) <sub>2</sub> NOCH <sub>3</sub> <sup>+</sup>	34.5	84	(CD <sub>3</sub> ) <sub>2</sub> NOCD <sub>3</sub>	34.9

The agreement of the relative intensities of our product mass peaks with those of the corresponding ions in the mass spectrum of the undeuterated compound, combined with the suggestion of Fig. 3 that  $m/e$  84 and 66 arise from the same compound, is convincing evidence that the product in our work is  $(CD_3)_2NOCD_3$ . This evidence is further strengthened by the fact that this product appears simultaneously with a concentration decrease of its likely precursor  $CD_3NO$  and does so in a vessel in which  $CD_3$  radicals are being formed at a constant rate. Adopting the conclusion that  $m/e$  66 and 84 are due to formation of  $(CD_3)_2NOCD_3$ , we can use the mass spectrum of  $(CH_3)_2NOCH_3$ <sup>3</sup> to correct the  $m/e$  48 peak for the contribution from  $(CD_3)_2NOCD_3$ . The corrected curve for  $m/e$  48, which is shown by the dotted line in Fig. 3, shows definitely that  $CD_3NO$  goes through a maximum rather than just reaching the steady state that is characteristic of a flow system.

To test our hypothesis that NO is practically completely consumed at or near the  $CD_3NO$  maximum, we carried out replicate photolyses on an azomethane- $d_6$ -nitric oxide mixture, one using an ionizing energy of 50 e.v. and the other a nominal ionizing energy of 18 e.v. At 18 e.v. ionizing energy  $m/e$  30 from azomethane- $d_6$  is reduced to less than 20% of  $m/e$  30 from nitric oxide, but there is still adequate sensitivity. The results are shown in Fig. 4, where the major portion of the plot shows the product peaks (ratioed to  $m/e$  64) as a function of photolysis time for an ionizing energy of 50 e.v. In the inset of Fig. 4 is shown the peak height of  $m/e$  30 at 18 e.v. as a function of time. The clear discontinuity near the maximum in  $m/e$  48 suggests, indeed, that at this point NO is effectively completely consumed. The further steady decrease of  $m/e$  30 after the maximum in  $m/e$  48 is attributed to the fact that near the maximum the major source of  $m/e$  30 at 18

(9) (a) C. S. Coe and T. F. Doumani, *J. Am. Chem. Soc.*, **70**, 1516 (1948);

(b) J. G. Calvert, S. S. Thomas, and P. L. Hanst, *ibid.*, **82**, 1 (1960).

(10) H. A. Taylor and F. P. Jahn, *J. Chem. Phys.*, **7**, 470 (1939).

(11) M. I. Christie, *Proc. Roy. Soc. (London)*, **A249**, 248 (1958).

(12) J. Collin, *Bull. soc. roy. sci. Liege*, **23**, 201 (1954).

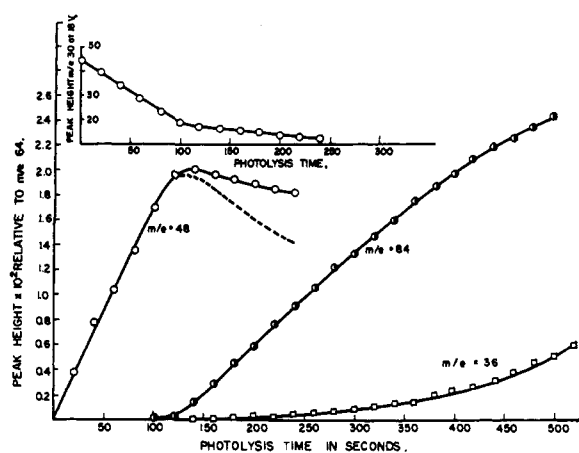


Fig. 4.—Growth of  $m/e$  36, 48, 84 at 50 e.v. and decay of  $m/e$  30 at 18 e.v.; initial  $[\text{NO}] \sim 0.2$  mm.

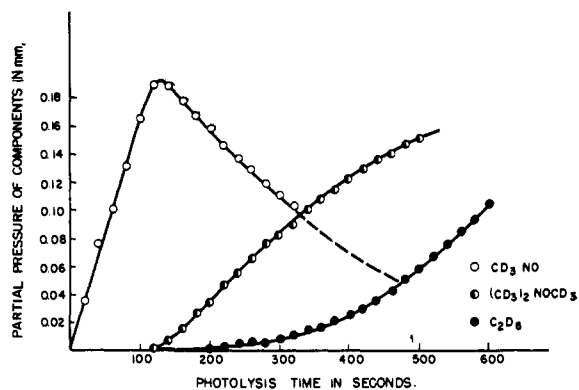


Fig. 5.—Partial pressures of  $\text{CD}_3\text{NO}$ ,  $(\text{CD}_3)_2\text{NO}$ , and  $\text{C}_2\text{D}_6$  as a function of irradiation time; initial  $[\text{NO}] \approx 0.2$  mm.

e.v. is  $\text{CD}_3\text{NO}$  rather than  $\text{NO}$ . As can be seen from the dotted line in Fig. 4, the concentration of this species is decreasing with photolysis time.

A further test of our hypothesis of nearly complete nitric oxide consumption can be made by considering the time required to reach the maximum ratio of  $m/e$  48 to 64 for various initial nitric oxide concentrations. Although it was not possible with the apparatus used to make up mixtures with accurately known initial nitric oxide concentration, let us assume, in accordance with our hypothesis, that the maximum value of the ratio of  $m/e$  48 to 64 is directly proportional to the initial oxide concentration. If our hypothesis is correct, the value of the ratio of  $m/e$  48 to 64 at the maximum should be approximately proportional to the time required to reach the maximum. For three photolyses at maximum peak height ratios ranging from  $3.8$  to  $11.4 \times 10^{-3}$ , this proportionality was found to hold within  $\pm 9\%$ . Since this is well within the reproducibility of the light intensity, we believe the proportionality is established. Thus our evidence leads us to conclude that the maximum in the growth curve of the  $m/e$  48 to 64 ratio corresponds to practically complete consumption of nitric oxide.

The conversion of mass spectral peak heights ratios to partial pressures was made by means of direct ethane and azomethane calibration, as described earlier, and the following assumptions: (1) for the same incident light intensity the initial rate of formation of  $\text{CD}_3\text{NO}$  is twice the initial rate of ethane- $d_6$  formation in the absence of nitric oxide; and (2) after depletion of nitric oxide,  $\text{NO}$  is present only as  $\text{CD}_3\text{NO}$  and  $(\text{CD}_3)_2\text{NOCD}_3$ ,

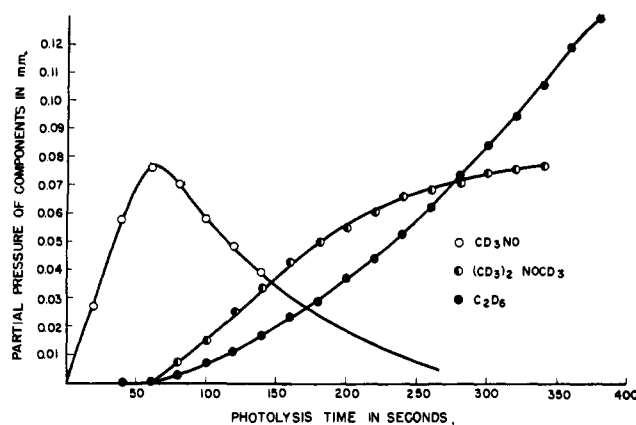


Fig. 6.—Photolysis of azomethane- $d_6$ -nitric oxide mixture; azomethane- $d_6$  pressure, 12.3 mm.; initial nitric oxide pressure, 0.98 mm.

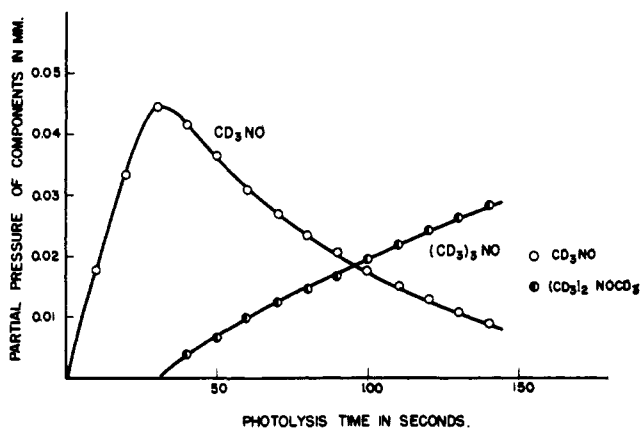
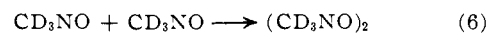
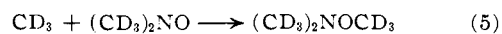
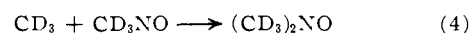
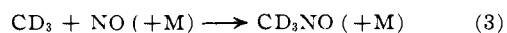


Fig. 7.—Photolysis of azomethane- $d_6$ -nitric oxide mixture; azomethane- $d_6$  pressure, 10.8 mm.; initial nitric oxide pressure, 0.04 mm.

so that the sum of the partial pressures of these two products is constant and essentially equal to the maximum partial pressure of  $\text{CD}_3\text{NO}$ .

The kinetic curves of product partial pressures as a function of photolysis time for three initial partial pressures of nitric oxide are shown in Fig. 5–7. As shown previously<sup>1</sup> the azomethane- $d_6$  partial pressure remains essentially constant over the photolysis times employed. As can be seen from Fig. 5–7, after the  $\text{NO}$  has undergone essentially complete conversion to  $\text{CD}_3\text{NO}$ , this product can no longer be formed and its concentration is then depleted while the concentration of  $(\text{CD}_3)_2\text{NOCD}_3$  increases but at a decreasing rate. The decreasing rate of formation of  $(\text{CD}_3)_2\text{NOCD}_3$  is in accord with one of its precursors being a substance whose concentration is continually decreasing, namely  $\text{CD}_3\text{NO}$ . On the other hand,  $\text{C}_2\text{D}_6$ , which is known to be formed by  $\text{CD}_3$  radical combination, is formed at an increasing rate which strongly suggests that the continually decreasing  $\text{CD}_3\text{NO}$  is competing for  $\text{CD}_3$  radicals. Thus, for the mechanism of the reaction in the presence of  $\text{NO}$ , we propose, in addition to 1 and 2, the reactions



We have not detected the species  $(\text{CD}_3)_2\text{NO}$  but this is not surprising for  $(\text{CD}_3)_2\text{NO}$  is a free radical formed

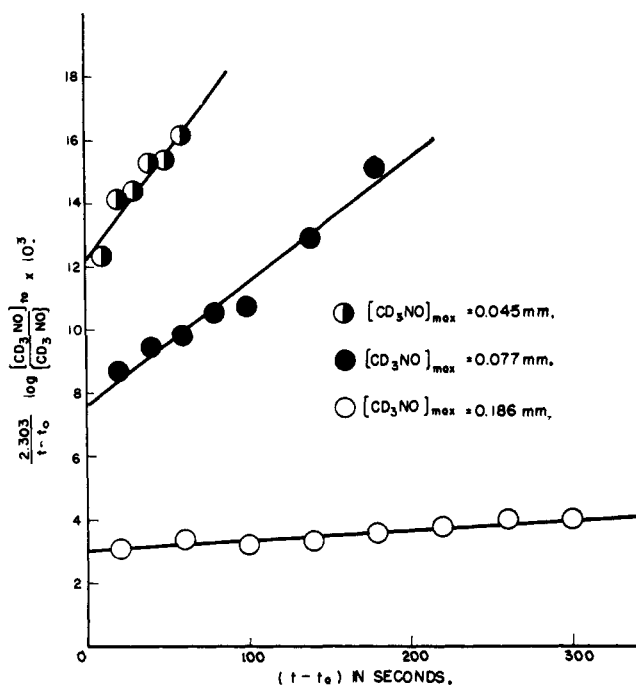


Fig. 8.—Kinetics of nitrosomethane- $d_3$  disappearance after the nitrosomethane- $d_3$  maximum.

"*in situ*" and cannot be expected, at the  $CD_3$  radical concentrations involved, to reach a detectable concentration in our system. As discussed earlier we have not detected the occurrence of 6 under our conditions. However, it is included in the mechanism since the estimated value of  $k_6^9$  and our lower limit to  $k_4$  (as shown later) are such as to suggest a contribution by 6 of the order of 5% to the total  $CD_3NO$  destruction at the highest  $CD_3NO$  pressure observed, namely 0.19 mm.

We can approximately evaluate the specific reaction rate of 4 by a kinetic analysis of the system after the  $CD_3NO$  maximum, that is after essentially complete depletion of  $NO$ , and with the assumption that 6 is negligible at the  $CD_3NO$  pressures obtaining in our system. This assumption is based upon our inability to detect 6, and upon the indication, using the estimated pertinent rate constants, that 6 makes only a minor contribution ( $\sim 5\%$ ) at the highest  $CD_3NO$  pressure in our experiments, a contribution which decreases as the  $CD_3NO$  pressure is lowered. Under these conditions the rate of depletion of  $CD_3NO$  is

$$-d[CD_3NO]/dt = k_4[CD_3][CD_3NO] + \lambda[CD_3NO] \quad (E4)$$

while the steady state concentration of  $CD_3$  after the  $NO$  is consumed is

$$[CD_3] = \frac{1}{4k_2} [(k_4^2[CD_3NO]^2 + 16\phi I_0\alpha[CD_3N=NCD_3])^{1/2} - k_4[CD_3NO]] \quad (E5)$$

By estimating  $(k_4/k_2^{1/2})$  from the relative slopes of the  $CD_3NO$  and  $C_2D_6$  partial pressure vs. time curves at various partial pressures of  $CD_3NO$  and using the value for  $k_2$  reported by Gomer and Kistiakowsky,<sup>13</sup> we arrive at an approximate value for  $k_4$ . With a value for  $k_4$  the steady state  $[CD_3]$  can be computed from E5 as a function of  $[CD_3NO]$ , and, hence, as a function of time, using the experimental curves in Fig. 5–7. When

(13) R. Gomer and G. B. Kistiakowsky, *J. Chem. Phys.*, **19**, 85 (1951).

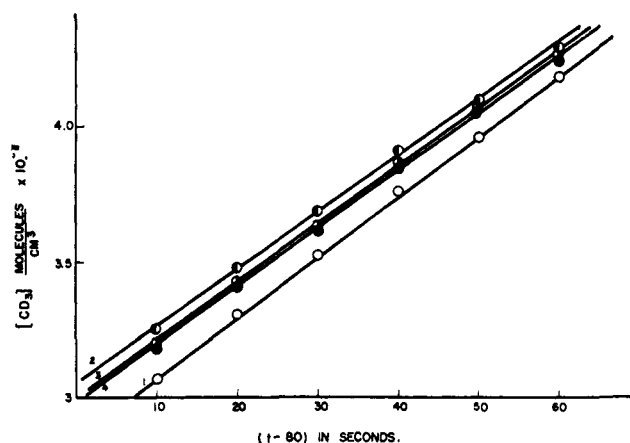


Fig. 9.—Iteration procedure for  $CD_3$  concentration. Small numbers on plot designate the iteration number.

this is done it is found that over an appreciable range of time, beginning with about 20 sec. past the  $CD_3NO$  maximum, the computed steady state  $[CD_3]$  is an approximately linear function of time. Hence we can write for this time range

$$[CD_3] = a + bt' \quad (E6)$$

where  $t'$  is the reaction time less some convenient time  $t_0$ , ( $t' = t - t_0$ ), and  $a$  and  $b$  are empirical constants determined by a plot of  $[CD_3]$  vs.  $t'$ . Substituting E6 into E4 and integrating, we have

$$\frac{1}{t'} \ln \frac{[CD_3NO]_0}{[CD_3NO]} = k_4a + \lambda + \frac{k_4b}{2} t' \quad (E7)$$

where  $[CD_3NO]_0$  is the nitrosomethane- $d_3$  concentration at  $t_0$ . Thus a plot of the left-hand side of E7 vs.  $t'$  should be linear with a slope of  $k_4b/2$  and an intercept of  $(k_4a + \lambda)$ . Such plots for three different initial concentrations of nitric oxide are shown in Fig. 8. Using the first values of  $a$  and  $b$  as determined by computation of  $[CD_3]$  from E5, a first-improved  $k_4$  can be computed. Then with the improved  $k_4$  the process using E5 can be repeated until successive iterations give no significant change in  $k_4$ . The linearity of the plots of  $[CD_3]$  vs.  $t'$  and the iteration procedure can be seen in Fig. 9 for the case of a mixture with an initial nitric oxide partial pressure of 0.044 mm.

Although, as can be seen from Fig. 8 and 9, each photolysis is internally consistent when analyzed by the treatment described, the values of  $k_4$  so calculated depend upon the initial nitric oxide concentration. The variation of the calculated  $k_4$  with initial nitric oxide concentration (or maximum  $CD_3NO$  concentration) is shown in Table II. This variation of  $k_4$  is without

$[NO]_0 \approx [CD_3NO]_{max}$ , mm.	$k_4$ , $cm.^3$ molecule $^{-1}$ sec. $^{-1} \times 10^{14}$
0.045	6.51
.077	4.57
.186	1.09

doubt due to the assumption of zero  $NO$  concentration after the  $CD_3NO$  maximum. In point of actual fact in such a flow system as ours the  $NO$  concentration cannot be zero because of the presence throughout the experiment of  $NO$  in the 3-l. reactant reservoir at its initial

*concentration.* The fact that the NO concentration in the photolysis cell becomes very small indicates simply that NO is being chemically consumed much faster than it leaks out of the photolysis cell into the mass spectrometer. The nitric oxide steady state concentration in the photolysis cell will therefore be proportional to the rate at which it diffuses into the cell from the reactant reservoir. After the  $\text{CD}_3\text{NO}$  maximum the NO concentration in the photolysis cell is very much less than the NO concentration in the reservoir, and therefore, the diffusion rate into the photolysis cell will be approximately proportional to the NO concentration in the reactant reservoir. The result is that, after the  $\text{CD}_3\text{NO}$  maximum, the steady state concentration of NO will be approximately proportional to the initial concentration of NO.

Although we cannot measure quantitatively the NO concentration, after the  $\text{CD}_3\text{NO}$  maximum, the rate of reaction 3 is sufficiently great<sup>4</sup> that the actual steady state concentration of  $\text{CD}_3$  will be influenced by the steady state NO concentration. Thus, because of reaction 3, the actual  $\text{CD}_3$  concentration will be a decreasing function of the initial nitric oxide concentration and in all cases will be lower than that calculated by E5; the difference between the actual and the calculated  $\text{CD}_3$  concentrations will, of course, diminish as the initial NO concentration is reduced. Since E5 overestimates the steady state  $\text{CD}_3$  concentration, the

treatment described underestimates  $k_4$ , with the amount of underestimation decreasing and becoming zero as the initial NO concentration approaches zero. Thus, the values of  $k_4$  in Table II are all lower limits to  $k_4$  and, in principle, the true value could be obtained by extrapolation of  $k_4$  to  $[\text{NO}]_0 = 0$ . Unfortunately,  $k_4$  is a complicated function of  $[\text{NO}]_0$  and our data do not permit a reliable extrapolation to be made. Nonetheless, we can say that  $k_4 > 6.51 \times 10^{-14}$  cm.<sup>3</sup>/molecule sec. and despite the uncertainty in the upper limit it is evident that 4 is a very fast reaction having a collision yield (assuming a collision diameter of 4.0 Å.) at 25° of  $1.9 \times 10^{-4}$ . The specific reaction rate of 4 is sufficiently high that the occurrence of 4 and 5 must be considered in the analysis of free radical reactions inhibited by nitric oxide. These reactions obviously will be of particular importance in nitric oxide inhibited reactions conducted over temperature ranges wherein  $(\text{CD}_3)_2\text{NO}$  and  $(\text{CD}_3)_2\text{NOCD}_3$  are thermally stable.

**Acknowledgment.**—We wish to thank Miss Kathleen Muller for her assistance with the calculations. This work was supported in part by the Petroleum Research Fund Grant 833-A1 and in part by contract AF33(616)-7716 with the Office of Aerospace Research. We are also pleased to acknowledge the assistance of the National Science Foundation in providing funds to aid in the purchase of the Bendix Time-of-Flight mass spectrometer.

[CONTRIBUTION FROM THE PARKINSON LABORATORY OF SOUTHERN ILLINOIS UNIVERSITY, CARBONDALE, ILL.]

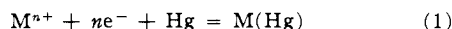
## The Influence of Ionic Strength on Polarographic Half-Wave Potentials. I. Aqueous Systems Involving Reversible Electrode Reactions and Amalgamation of the Reduced Species in Uni-univalent Inert Electrolytes

BY DOUGLAS E. SELLERS AND NICHOLAS E. VANDERBORGH

RECEIVED NOVEMBER 6, 1963

A method for the mathematical estimation of the change in the observed half-wave potential of a metal ion with changes in the concentration of the inert (supporting) electrolyte is derived. A method for the correlation of half-wave potentials in systems of high ionic strength and for the correction of polarographically determined dissociation constants (where the ionic strength is maintained constant by varying the concentrations of different ionic species) is implied.

For the polarographic investigation of simple metal ions, the reduction to the metallic state (amalgams) has been represented<sup>1</sup> simply as



where  $\text{M}^{n+}$  represents the simple, hydrated metal ion. The potential of the dropping electrode, when the reaction is rapid and reversible, is given<sup>1</sup> by

$$E_{d.e.} = E_a^\circ - \frac{RT}{nF} \ln \frac{C_a^0 y_a}{a_{\text{Hg}} C_s^0 y_s} \quad (2)$$

where  $C_a^0$  and  $C_s^0$  are the molar concentrations of the reduced or reducible species in the amalgam and solution at the surface of the drop, respectively; the terms  $y_a$  and  $y_s$  are the corresponding molar activity coefficients and  $a_{\text{Hg}}$  is the activity of the mercury. The corresponding representation of the half-wave potential, considering the effect of the liquid junction potential,

has been given<sup>2</sup> as

$$E_{1/2} = \epsilon - E_L + \frac{RT}{nF} \ln y_s - \frac{RT}{2nF} \ln (D_s/D_a) \quad (3)$$

where  $D_a$  and  $D_s$  are the diffusion coefficients of the metal in mercury and in solution, respectively; the constant  $\epsilon$  is equal to  $E_a^\circ - RT/nF \ln (y_a/a_{\text{Hg}})$ .

However, if polarographic measurements are to be carried out in aqueous systems of high concentrations of inert electrolyte, a question arises as to the constancy of the activity of water, as is assumed in the statements of eq. 1 and 3, the influence of the high ionic strength on  $y_s$ ; the magnitude of the change of  $E_L$ <sup>2</sup>; the liquid junction potential, as well as other factors.<sup>3</sup> It appears doubtful that such simplifying assumptions which are made in the usual derivation of eq. 3 are valid in such instances and has been illustrated by DeFord and Anderson.<sup>2</sup>

(2) D. D. DeFord and D. L. Anderson, *J. Am. Chem. Soc.*, **72**, 3918 (1950).

(3) W. B. Schaap, *ibid.*, **82**, 1837 (1960).

(1) I. M. Kolthoff and J. J. Lingane, "Polarography," 2nd Ed., Interscience Publishers, Inc., New York, N. Y., 1952.